

# The flocs generator reactor-FGR: a new basis for flocculation and solid–liquid separation

E. Carissimi, J. Rubio\*

*Departamento de Engenharia de Minas, Laboratório de Tecnologia Mineral e Ambiental (LTM)-PPGEM-Universidade Federal do Rio Grande do Sul, Av. Osvaldo Aranha, 99/512, Porto Alegre RS 90035-190, Brazil*

Received 9 March 2004; received in revised form 12 August 2004; accepted 12 August 2004

## Abstract

This work presents the design and the basic development of an innovative in-line mixing helical (coiled) reactor for the flocculation and solid–liquid separation of suspended particles. The device system was named flocs generator reactor (FGR), a compact flocculation system whereby the flocculation of particles is assisted by the kinetic energy transfer from the hydraulic flow through the reactor. The flow mixing, characterized as a plug flow regime with a slow dispersion, promoted the required hydrodynamics conditions to disperse the polymer flocculant (cationic polyacrylamide) and also to generate “strong” flocs of  $\text{Fe}(\text{OH})_3$  (colloidal suspension model system) at pH 7.5. The solid–liquid separation of the flocs was then achieved either by settling or by flotation with microbubbles (30–70  $\mu\text{m}$ ). Studies were carried out with different models of FGRs (varying the length/volume ratio), and process efficiency (mainly kinetics) was evaluated as a function of polymer concentration and operating parameters, namely, feed flow rate, air-to-solids ratio and residence time. Results showed that the aerated flocs are readily floated with rising rates of the order of  $120 \text{ m h}^{-1}$ , values higher than those obtained for the settling of the nonaerated flocs ( $18\text{--}24 \text{ m h}^{-1}$ ). The FGR requires short residence times and generates dense, well-structured flocs (with a mass fractal dimension,  $d_F$  of about 3) which withstand high shear forces. Due to the high process efficiency and high loading capacity shown, it is believed that the FGR has a good potential as an in-line flocculation (or flotation) separator device in applications requiring high rate solid–liquid separations.

© 2004 Elsevier B.V. All rights reserved.

**Keywords:** flocculation; coiled reactor; solid–liquid separation; effluents treatment

## 1. Introduction

Flocculation is a known process employed worldwide in several industrial operations, among others, thickening, wastewater treatment, mineral processing and papermaking (Yeung and Pelton, 1996; Yeung et al., 1997; Thomas et al., 1999; Biggs et al., 2000; Agarwal, 2002; Porubská et al., 2002). The purpose of

\* Corresponding author. Tel.: +55 513316 3540; fax: +55 51 3316 3530.

E-mail address: [jrubio@ufrgs.br](mailto:jrubio@ufrgs.br) (J. Rubio).

URL: <http://www.lapes.ufrgs.br/ltn>.

flocculation in wastewater treatment is to form strong aggregates from finely divided solid particles or oily droplets before separation by settling or flotation (Rubio et al., 2002; Rubio, 2003). The properties of flocs produced from flocculation step prior to solid–liquid separation are crucial in determining the overall efficiency of water or wastewater treatment processes.

Flocculation of suspended particles takes place after polymer diffusion and adsorption under stirring (agitation), followed by flocs build-up and growth at slow mixing stage. The bigger the floc, the faster is the solid–liquid separation settling rate (Bratby, 1980; Weir and Moody, 2003). This might not be necessary in the flotation of the flocs (floc flotation) whereby other phenomena operate, i.e., bubble attachment, entrainment and entrapment (Rubio et al., 2002; Rubio, 2003).

Usually, flocculation is performed in agitated tanks or basins, and although appears to be quite simple, the process (and the devices) still presents problems such as short circuits, dead zones, high mechanical and electrical energy requirement, fairly high maintenance costs, etc. According to Bhole (1993), even mechanical flocculators require paddles, shaft, bearings, gear box system, motor, energy and skilled process supervision, all enhancing the operating costs.

Yet, coagulation and flocculation may be conducted in in-line mixing facilities, such as conduits and pipes connecting treatment units (Metcalf and Eddy, 2003). The main advantage of using in-line units is the possibility of taking advantage of the kinetic energy transfer of the hydraulic fluid to promote the agitation needed to disperse a destabilizing agent and for the generation of aggregates along the unit. Furthermore, the use of in-line mixing facilities dispenses the use of mobile parts (agitators), presents a residence time distribution close to a plug flow reactor (less short circuits or dead zones), low installation costs, simple design (smaller foot-print area) with reduced mechanical and electrical energy consumption.

According to Gregory (1988) and Yukselen and Gregory (2003), the process of flocculation may be considerably influenced by the intensity of the applied shear force. The hydrodynamic forces influence the polymer adsorption phenomena and the collision

efficiency among particles, determining the overall rate of flocculation (Agarwal, 2002; Metcalf and Eddy, 2003). Although mixing increases the collision frequency of particles during floc formation process, the shear forces might cause flocs fragmentation (Weir and Moody, 2003; Yukselen and Gregory, 2003). This intensity of mixing is mainly characterized by the velocity gradient ( $G$ ), which measures the velocity of the fluid spatially (from point to point) (Weber, 1972; Cleasby, 1984). However, the criteria for determining optimal flocculation conditions depend on the specific application (Yeung et al., 1997). As a rule, the flocs must be strong enough to withstand an adequate solid–liquid separation step and/or a sludge dewatering process.

Curved configurations of circular tubes, such as bends, and helical coils are commonly found in the industry mainly in heat exchangers, chemical reactors, reverse osmosis units (Agrawal and Nigam, 2001) and enzymatic polymerization reactors (Buchanan et al., 1998). Several authors (Streeter, 1961; Gregory, 1981, 1987; Hüttel and Friedrich, 2000; Agrawal and Nigam, 2001) have shown some advantages presented by the secondary flow induced by centrifugal forces when a flow passes through curved pipes, which cause a movement toward the outside of the curve, giving more flocculation than that in a straight tube. According to Austin and Seader (1973), the hydrodynamics in a coiled pipe is also largely characterized by the magnitude of the critical Reynolds number which can be four (4) times greater than that in a linear tube.

Despite the advantages presented by coiled pipe facilities in numerous industrial processes, there is no much information about the employment of these units for the flocculation of suspended solids in water and wastewater applications. Only a few authors have evaluated in-line coiled mixing units for the generation of flocs at laboratory scale, namely, flocculation of polystyrene latex particles (Gregory, 1981, 1987), dried yeast cells (Gregory, 1988), synthetic bentonite suspension (Elmaleh and Jabbouri, 1991) and the treatment of a synthetic effluent (Odegaard et al., 1992).

Therefore, the aim of the present paper was to describe the design and basic development of a new compact in-line coiled reactor to flocculate and separate suspended particles. The flocculation reactor

behaves actually as a contactor and was named flocs generator reactor-FGR, and its efficiency was evaluated using colloidal  $\text{Fe}(\text{OH})_3$  as a solid model (disperse particles) and a cationic polyacrylamide as the flocculant. The solid–liquid separation was evaluated comparing the rate of flocs settling with the flocs flotation after addition (injection) of microbubbles of controlled size (FGR as aerated flocs generation device).

## 2. Experimental

### 2.1. Materials

#### 2.1.1. Reagents

The reagents employed were  $\text{FeCl}_3 \cdot 6\text{H}_2\text{O}$  (Synth<sup>TM</sup>) for the generation of the colloidal precipitates,  $\text{Ca}(\text{OH})_2$  for the pH adjustments and a high molecular weight cationic polyacrylamide (Mafloc 490 C<sup>TM</sup>) supplied by SNF/Floerger<sup>TM</sup>. Methylene blue supplied by Nuclear<sup>TM</sup> was used in the studies of the dispersion as a tracer. All reagents used were of analytical purity, and the experiments were carried out with tap water.

#### 2.1.2. Equipment

The flocs generator reactor-FGR was designed and constructed for flocs generation ahead to the solid (flocs)–liquid separation stage, with feed rates ranging from 0.12 to 0.6  $\text{m}^3 \text{h}^{-1}$  (2 to 10  $\text{lmin}^{-1}$ ). The semipilot scale FGR (Fig. 1) was constructed with a polyurethane pipe with an inner diameter of 1.25 cm, enrolling a 10 cm diameter polyvinyl chloride (PVC) column.

Four (4) different reactor models with varying length/volume ratios were evaluated for the generation

Table 1

Constructive parameters of the reactors used for the flocs generation

Reactor	Number of rings	Length (m)	Volume (l)
FGR 1	16	6	0.6
FGR 2	32	12	1.2
FGR 3	48	18	1.8
FGR 4	64	24	2.4

of the flocs. The constructive characteristics are summarized in Table 1.

The system rig used, shown in Fig. 2, is composed of two tanks (capacity of 500 l each) for the  $\text{Fe}(\text{OH})_3$  preparation and storage, two helical pumps, a Nestzsch<sup>TM</sup> model 2NE30A to feed the in-line mixing unit and a Nestzsch<sup>TM</sup> model 2NE15A to feed the saturator vessel with tap water.

The feed rate was controlled by a Weg<sup>TM</sup> frequency controlling equipment model CFW 07. A Masterflex<sup>TM</sup> (model 7518-10) dosing peristaltic pump with a Tygon<sup>TM</sup> tubing model 6409-13 was used to inject the polymer. For the generation of the microbubbles (as in dissolved air flotation [DAF]), air was dissolved into water using a saturator vessel (90 cm in height and 10 cm in diameter). The saturator, operating at varying pressures (2, 3, 4, 5 and 6 atm), was constructed with a bed height of 50 cm, filled with pall rings of 25 mm in height and 25 mm in diameter.

### 2.2. Methods

Flocculation experiments were carried out at room temperature, using colloidal  $\text{Fe}(\text{OH})_3$  dispersion formed from the  $\text{FeCl}_3 \cdot 6\text{H}_2\text{O}$  dissolution and subsequent precipitation with  $\text{Ca}(\text{OH})_2$  at  $\text{pH } 7.5 \pm 0.5$  (monitored with an Analion<sup>TM</sup> pHmeter, model PM 608). The Mafloc 490 C<sup>TM</sup> polymer was added in-line to the  $\text{Fe}(\text{OH})_3$  aqueous dispersion and pumped to the FGR for the flocs generation (aerated or nonaerated ones).

The flow exiting from the FGR fed the solid–liquid separation vessels (columns) whereby the settling (non aerated flocs) and up rising (aerated flocs) rates were evaluated. These rates were calculated, monitoring the times needed for the flocs to travel a fixed distance. Time measurements were made by direct observations (randomly) of many individual flocs. Also, flocculation efficiency was

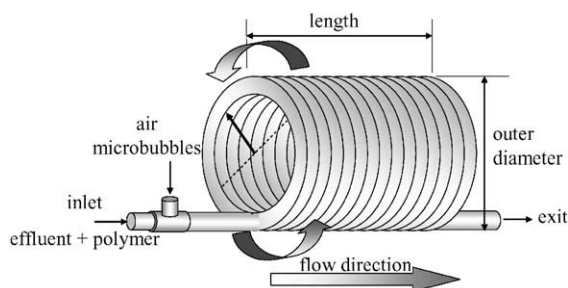


Fig. 1. Flocs generator reactor (FGR) unit.

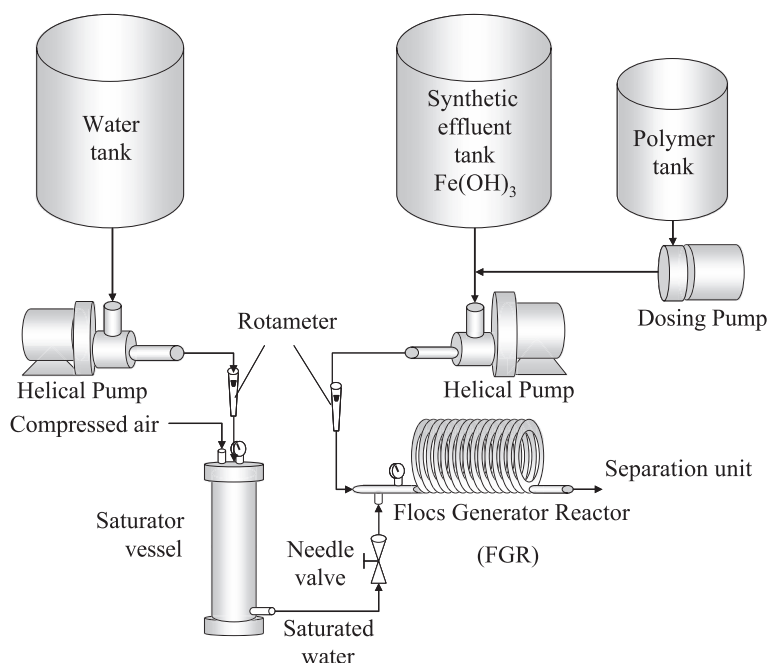


Fig. 2. System rig used for the flocs generation in the FGR.

monitored by means of the iron removal from water analysing, with a Varian<sup>™</sup> atomic absorption spectrometer, the residual iron concentration in the supernatants after flocculation. In all cases, the flocculation degrees were higher than 95%.

The evaluation of the performance of the flocs generator reactor (FGR) and its optimization were made by monitoring the separation rate of the flocs formed. The criterion used (for optimal conditions) was the faster separation rates, settling time of non aerated flocs and up rising rate of the aerated ones.

All experimental conditions were tested in triplicate, with at least 25 times measurements of separation in each experimental set. An arithmetic medium of all the values obtained were calculated and statistically analysed according to the analysis of variance (one-way ANOVA), as described in Montgomery (1991).

#### 2.2.1. Studies with nonaerated flocs

In the measurements of the nonaerated flocs settling rates, 1 l of sample exiting the FGR was introduced in a graduated cylinder. The density of these flocs was calculated using the Stokes law for

laminar flux, using the settling rates data and the size of the flocs. The latter were obtained from photographic analysis (using a Sony<sup>™</sup> digital camera, model DSC) and sized with a graduated scale (fixed at the same cylinder).

The mass fractal dimension of the flocs was obtained using settling rate and size data obtained from settling experiments and through logarithmic correlation between the mass and the size of the flocs, considering spherical geometry (Gregory, 1988, 1998; Tang et al., 2002).

#### 2.2.2. Studies with aerated flocs

In the experiments carried out with aerated flocs, microbubbles with sizes ranging from 30 to 70  $\mu\text{m}$  (Rodrigues and Rubio, 2003) were introduced in the inlet of the FGR. The air employed in the saturator vessel was supplied by an air compressor, and the microbubbles were generated by the depressurization of the air-saturated solution under controlled pressure through a nozzle (needle valve), in the same manner as in the dissolved air flotation-DAF (Edzwald, 1995; Liers et al., 1996; Kiuru, 2001; Rubio et al., 2001). The injection of the micro-

bubbles into the FGR is followed by entrainment and/or entrapment of these bubbles onto (or into) the  $\text{Fe}(\text{OH})_3$  polymer flocs, forming the so-called “aerated” flocs.

The solid–liquid separation of these floating flocs was measured monitoring the up rising times in a graduated cylindrical column.

Studies of the effect of the air/solids ratio on the separation efficiency were conducted fixing the ratio of injection of microbubbles in 10% and varying the saturation pressure (2, 3, 4, 5 and 6 atmospheres). The calculation of the air-to-solids ratio was made using the following Eq. (1).

$$as = \frac{Ri \cdot Av}{FR \cdot [sol]} \cdot S \quad (1)$$

where as=air/solids ratio ( $\text{mlmg}^{-1}$ ); Ri=rate of injection of microbubbles ( $\text{lmin}^{-1}$ ); Av=theoretical volume of dissolved air per litre of water, according to the Henry law ( $\text{mll}^{-1}$ ); FR=feed rate ( $\text{lmin}^{-1}$ ); S=saturator vessel efficiency (%).

### 2.2.3. Studies of the hydrodynamic flow in the FGR

The axial dispersion model in the FGR was evaluated using a tracer with an instantaneous (short term) injection of 1 ml of 10,000  $\text{mg l}^{-1}$  of methylene blue solution. Samples of the outlet flow were collected every 5 s and stored in polyethylene flasks. Methylene blue concentration was measured by molecular absorption using a Merck<sup>™</sup> spectrophotometer (model SQ 118) at a wavelength of 660 nm. The experiments were carried out in triplicate, and the result showed is an arithmetic average of the data obtained.

The velocity gradient was calculated from the head loss in the FGR with varying feed rates applying Eq. (2). Measurements were made using manometers between the FGR inlet and the outlet flows (the head loss at the entrance was negligible).

$$G = \sqrt{\frac{\gamma \cdot Hl}{\mu \cdot t}} \quad (2)$$

where:  $G$ =velocity gradient ( $\text{s}^{-1}$ );  $\gamma$ =specific weight of water ( $998.2 \text{ kgf m}^{-3}$  at  $20^\circ\text{C}$ );  $Hl$ =head loss (m);  $\mu$ =absolute viscosity of water ( $1.029 \times 10^{-4} \text{ kgf s m}^{-2}$  at  $20^\circ\text{C}$ );  $t$ =time (s).

The Reynolds number determination was calculated from Eq. (3), where  $V$  is the flow velocity,  $D$  is the tube diameter, and  $\mu$  is the kinematic viscosity of the solution.

$$Re = \frac{V \cdot D}{\mu} \quad (3)$$

## 3. Results and discussion

### 3.1. The formation of flocs in the FGR and their settling rate

The effect of the reactor type and the feed rate on the settling rate of the flocs generated is shown in Fig. 3.

For all the reactors types, the highest settling rates ranged from 12 to 19  $\text{m h}^{-1}$ , showing an optimal for a feed rate of 4  $\text{lmin}^{-1}$  (or residence time, as shown in Fig. 4). At the smaller feed rates (2  $\text{lmin}^{-1}$ ), the low efficiency may be due the low turbulence required to form the flocs, especially with high molecular weight polymeric flocculant, such as the Mafloc 490 C<sup>™</sup> (Weir and Moody, 2003). For the very high feed rates, the system turbulence contributed to the rupture of the flocs now decreasing their settling rate.

The residence time of the different reactors as a function of the feed flow rates is shown in Fig. 4.

Following the results obtained, the FGR 2, which showed the highest settling rates (19  $\text{m h}^{-1}$ ) and

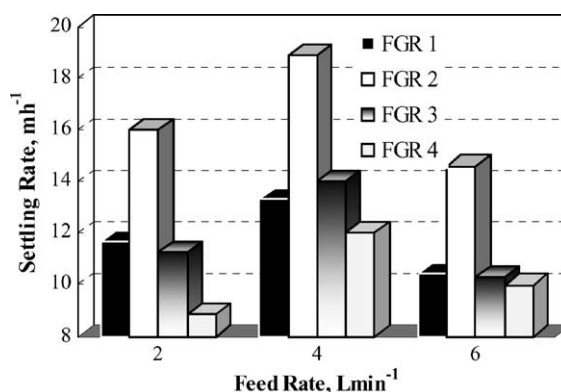


Fig. 3. Flocs settling rates as a function of feed rate and FGR model. Conditions,  $[\text{Fe}(\text{OH})_3]=58 \text{ mg l}^{-1}$ ,  $[\text{Mafloc 490 C}]=5 \text{ mg l}^{-1}$ ,  $\text{pH } 7.5 \pm 0.5$ .



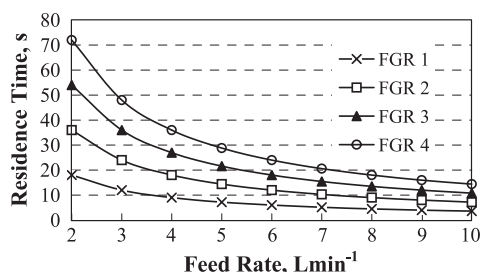


Fig. 4. Residence times at different FGR models as a function of the feed rate.

yielded large flocs (4–8 mm), was selected for further investigation.

Fig. 5 shows the effect of the feed rate and residence time in the flocs settling rates. Results show that an increase in the inlet flow rate decreases the settling rate of the flocs generated. This may be attributed to the high turbulence (determined by the system hydrodynamic conditions), which led to the rupture of the formed flocs in the reactor. Other authors (Akers et al., 1987) have already investigated the effect of turbulent conditions in tubular systems by observing the rupture of the flocs generated using small latex particles (0.97  $\mu\text{m}$ ). According to these authors, the rupture of the flocs is highly dependent on the level of the dissipated energy with turbulence. Moreover, the density distribution of the flocs or the conditions where these flocs are formed may interfere in their resistance.

Fig. 5 also shows the increase in the flocs settling rates with the increase in the residence time. The results obtained show that for a residence time up to 10 s, the increase in the settling rate is not as

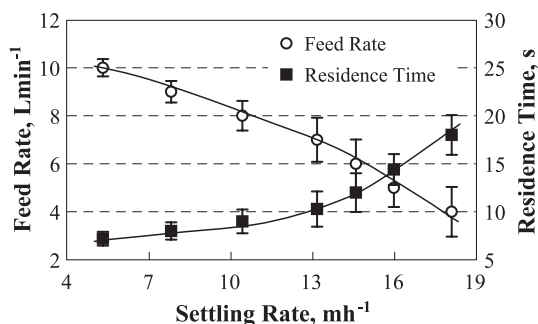


Fig. 5. Settling rate of the flocs as a function of the feed rate and residence time. Conditions,  $[\text{Fe}(\text{OH})_3]=58 \text{ mg l}^{-1}$ ,  $[\text{Mafloc 490 C}]=5 \text{ mg l}^{-1}$ , FGR 2.

meaningful as for times higher than 10 s. This is probably due the fast interaction between particles and polymer adsorption onto particles promoted by turbulence in the FGR. In fact, according to Weber (1972), the polymer adsorption onto particles is very rapid and irreversible.

The settling rates of the  $\text{Fe}(\text{OH})_3$  flocs obtained for different polymer (Mafloc 490 C<sup>TM</sup>) concentrations is shown in Fig. 6. The results show that the settling rate increased at higher polymer concentrations due the formation of larger flocs, as observed by other authors in other systems (Adachi and Tanaka, 1997; Gregory, 1997). However, the flocs do not continue to grow indefinitely in size during prolonged shearing and polymer addition; instead, they attain an equilibrium size. Hence, for concentrations higher than  $5 \text{ mg l}^{-1}$ , the increase in settling rates was not significant, and for this reason, this polymer concentration was chosen for further studies.

Gregory (1988) evaluated comparatively the flocculation efficiency monitoring the polymer adsorption onto yeast dried cells suspension at a concentration of  $1 \text{ g l}^{-1}$  in a batch reactor and in a continuous reactor. In batch tests, the suspension was stirred during 1–2 min using a magnetic stirrer and sampled at a rate of  $5 \text{ ml min}^{-1}$ . In the continuous tests, the yeast suspension and the polymer were mixed and flowed through a 1 m of coiled 1-mm-diameter tubing (volume of 0.8 ml) at a flow rate of  $10 \text{ ml min}^{-1}$ , with a residence time lesser than 5 s. According to this author, despite the short residence time in the tube, there were enough particle collisions to give a degree of flocculation similar to that occurring after 1–2 min in a stirred beaker. However, the particles destabilization depends

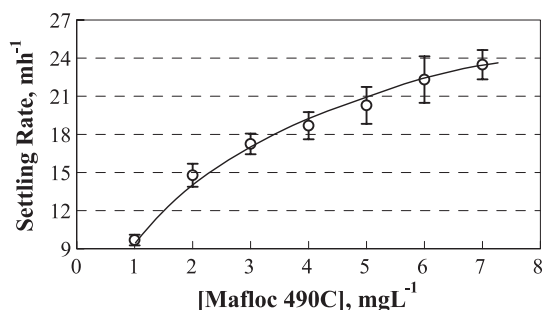


Fig. 6. Settling rate of the flocs as a function of the polymer Mafloc 490 C<sup>TM</sup> concentration. Conditions,  $[\text{Fe}(\text{OH})_3]=58 \text{ mg l}^{-1}$ , pH  $7.5 \pm 0.5$ , feed rate  $=3 \text{ l min}^{-1}$ , FGR 2.

much on the polymer employed, and sometimes, the tubular system required a polymer dosage higher than in the batch system.

### 3.2. Flocs characterization

Results of physical characterization of the flocs generated in the FGR are shown in Figs. 7 and 8, respectively. Fig. 7 shows that the flocs density decreases considerably as the flocs size increase due the flocs fractal dimension, as previously described by other authors (Klimpel and Hogg, 1991; Adachi and Tanaka, 1997; Gregory, 1997; Tang et al., 2002). The average value of the density of the  $\text{Fe}(\text{OH})_3$  flocs generated in the reactor was  $1019 \pm 18 \text{ kgm}^{-3}$  for flocs with sizes ranging from 400 and 2000  $\mu\text{m}$ .

Larue and Vorobiev (2003) utilized settling data of  $\text{Fe}(\text{OH})_3$  flocs (obtained using optical microscopy) to calculate the diameter and density of the flocs through Stokes law. Thus, for a concentration of  $800 \text{ mg l}^{-1}$  of  $\text{Fe}(\text{OH})_3$ , the authors obtained an average diameter of flocs of  $213 \pm 4 \mu\text{m}$  and an average density of  $1026.4 \text{ kgm}^{-3}$ . The density value obtained by these authors is within the range of values of densities obtained for the flocs generated in the FGR (Fig. 7).

The mass fractal dimension ( $d_F$ ) of the  $\text{Fe}(\text{OH})_3$  flocs obtained in this work is shown in Fig. 8. The value obtained of  $d_F$  (2.98) characterizes a dense floc, with low porosity and spherical format. Values of about 3 have been already reported in the literature and were explained as a result of linear trajectories, yielding more compact and spherical structures also called as “ballistic” aggregation, which happens mainly in the particle–cluster case of aggregation (Gregory, 1997; Burns et al., 1997, 1998).

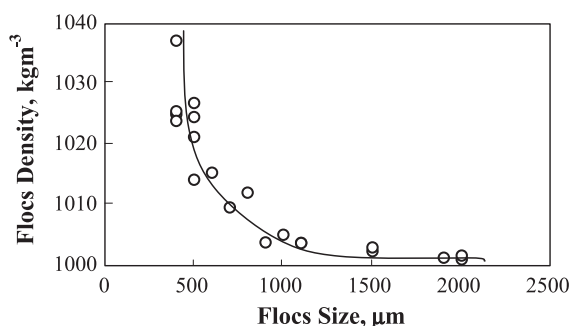


Fig. 7. Density of the flocs as a function of  $\text{Fe}(\text{OH})_3$  flocs size. Conditions,  $[\text{Fe}(\text{OH})_3]=58 \text{ mg l}^{-1}$ , FGR 2, pH  $7.5 \pm 0.5$ .

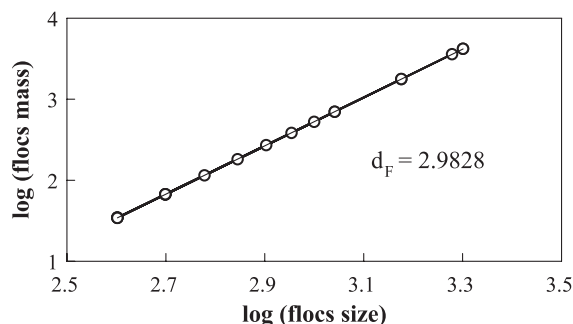


Fig. 8. Fractal dimension of  $\text{Fe}(\text{OH})_3$  flocs. Conditions,  $[\text{Fe}(\text{OH})_3]=58 \text{ mg l}^{-1}$ ,  $[\text{Mafloc 490 C}]=5 \text{ mg l}^{-1}$ , FGR 2, pH  $7.5 \pm 0.5$ .

Yet, the FGR, because of its coiled design, presents some peculiarities, among others, a fairly good shear rate for aggregation, a secondary flow and centrifugal collision operating forces. These properties enable a good contact between the high molecular weight polymer macromolecules and the colloids and thus form strong, big and compact structures.

### 3.3. FGR characterization

The hydraulic performance of the reactor is shown in the Fig. 9 by the tracer (methylene blue) response curve. The analysis of the concentration of the dye versus time shows an intense peak close to 24 s (theoretical residence time of the FGR 2) for a flow inlet of  $3 \text{ l min}^{-1}$ . The methylene blue mass recovery was estimated in about 80%. The peak presents a slow tracer scattering mainly due the turbulent mixing of the flow inside the FGR, characterizing a plug flow regime with a slow dispersion (Levenspiel, 1999).

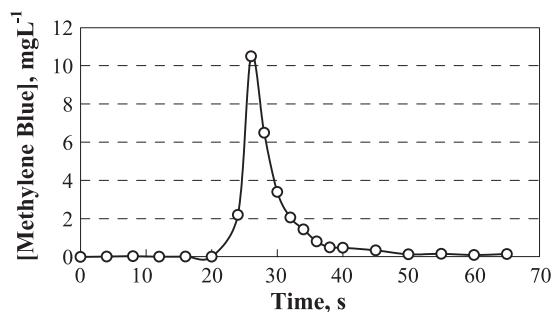


Fig. 9. Response curve of the tracer along the FGR. Conditions, feed rate  $=3 \text{ l min}^{-1}$ ,  $[\text{methylene blue}]=10,000 \text{ mg l}^{-1}$ , FGR 2.

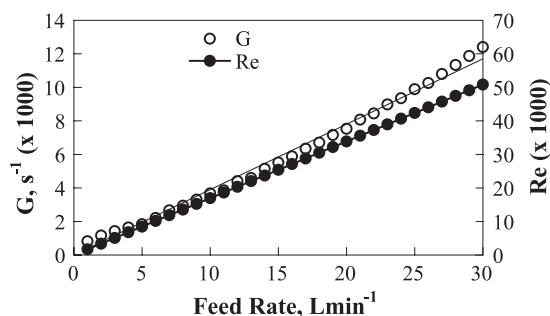


Fig. 10.  $G$  and  $Re$  values as a function of the feed rate in the FGR.

The velocity gradient ( $G$ ) and the Reynolds number ( $Re$ ) data calculated from the feed rate (1 to 30  $\text{lmin}^{-1}$ ) are shown in Fig. 10. Inlet feeds higher than 3  $\text{lmin}^{-1}$  yielded  $Re$  values characterizing a turbulent mixing and  $G$  values higher than 1400  $\text{s}^{-1}$  which enable a good mixing for the polymer adsorption at the colloidal precipitates/solution interface. Moreover, the secondary flow at high feed rates causes a high energy dissipation requiring higher pressures to drive the fluid through the coiled tube than that needed in a straight tube having the same length and flow rate. At lower flow rates this extra dissipation is negligible, but a secondary flow has another important effect. In a curved tube, the flow is subject to centrifugal forces making particles to remain longer times in the tube than those located near the center of a straight tube. According to Gregory (1987), this coiled flow presents a more uniform  $Gt$  distribution, resulting in a better flocculation than that in a straight tube.

### 3.4. The formation of aerated flocs and their flotation

In this system, not only the flocculation is favored (higher turbulence) but also the entrainment and/or entrapment of the air bubbles inside the flocs leading to formation of big aerated units. This phenomenon was observed visually and is represented schematically in Fig. 11. Thus, the aerated flocs “float” and are easily separated as a flotation (or floatation) product (or floc flotation). Therefore, the FGR, in this case, serves at the same time as a flocculator and as an air bubble/floc contactor.

The effect of the reactor type was again evaluated through the determination of the flocs up rising rates using the technique already described (results are shown in Fig. 12).

In all reactors, the highest up rising rates were obtained for the feed rate of 2  $\text{lmin}^{-1}$ , with values ranging from 67 to 112  $\text{m h}^{-1}$ . For feed rates above 2  $\text{lmin}^{-1}$ , there was a decrease in the up rising rate due to the increase in turbulence caused by the increase of the inlet flow rate and the injection of the microbubbles. However, using FGR 2, the difference in the up rising rates of the flocs for the feed rates investigated is not so meaningful.

FGR 2 presented (again) the best results in terms of floc up rising rate (112  $\text{m h}^{-1}$ ), and this reactor was chosen for further tests. FGR 1 showed poor efficiency due the short length, which did not allow a sufficient residence time for the flocs formation. FGRs 3 and 4 presented a decrease in the up rising rates probably due the rupture of the flocs for all the

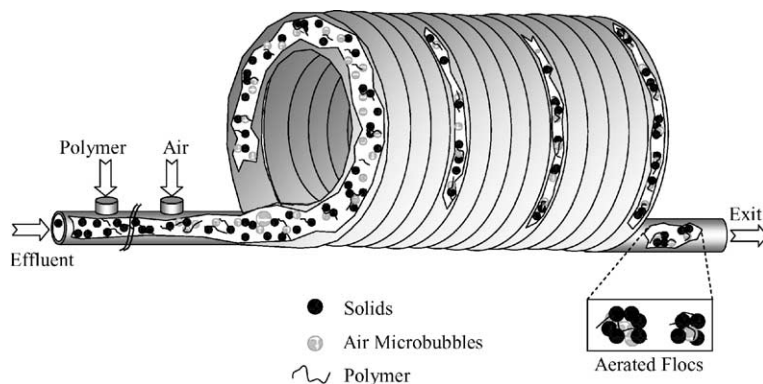


Fig. 11. Generation and growing of aerated flocs inside the FGR.



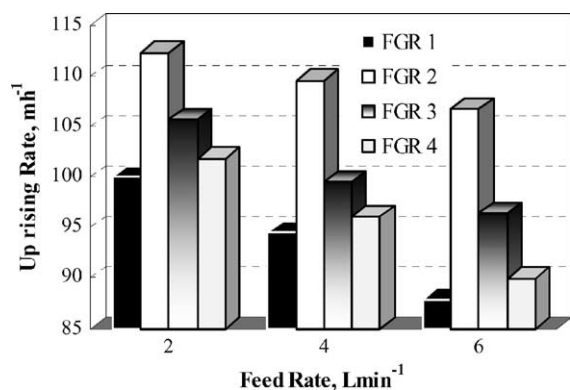


Fig. 12. Up rising rate of the flocs as a function of feed rate and FGR type. Conditions,  $[\text{Fe}(\text{OH})_3]=58 \text{ mg l}^{-1}$ ,  $[\text{Mafloc 490 C}]=5 \text{ mg l}^{-1}$ , air injection ratio=50%, pH  $7.5 \pm 0.5$ .

feed rates. As previously mentioned, flocs do not continue to grow indefinitely during prolonged shearing, but they attain an equilibrium size instead.

The variation of the flocs up rising velocity according to the air to solids ratio is shown in the Fig. 13.

Fig. 13 shows that best results are obtained with an air/solids ratio greater than  $0.025 \text{ ml mg}^{-1}$ . Previous studies of flotation of colloidal iron flocs showed removal of iron efficiencies higher than 80% with an air/solids ratio of 0.5 (Shannon and Buisson, 1980). Results obtained in this work at lower air/solids ratio may be explained in terms of the better efficiency of collision, adhesion, entrainment and entrapment of bubbles inside or onto the flocs, which does not occur in a conventional process of dissolved air flotation. According to Purchas (1977), the values of the air/solids ratio are more

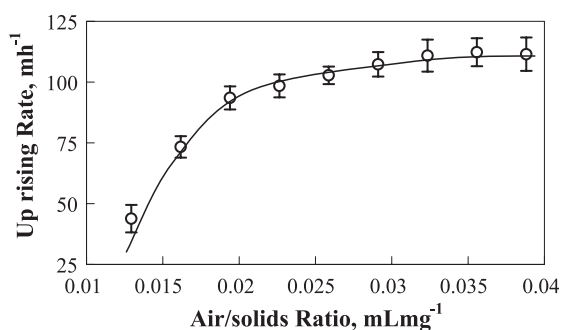


Fig. 13. Up rising rate of the flocs as a function of the air/solids ratio. Conditions,  $[\text{Mafloc 490 C}]=5 \text{ mg l}^{-1}$ , FGR 2, pH  $7.5 \pm 0.5$ .

related to the amount of air precipitated and not to the quantity of air bubbles actually adhered to the floating particles. Thus, the results obtained validate the good function of the FGR as a bubble/particle contactor, enabling the use of air/solids ratio values much lower than those utilized in conventional processes.

Comparative results obtained in this work revealed that the separation rates of the aerated flocs are of the order of six times higher than the flocs settling. The floating rates of the aerated flocs (5–8 mm), reaching values higher than  $100 \text{ m h}^{-1}$ , result from the air volume inside the floc structure plus the volume given by the adhered bubbles at the floc/water interface. Accordingly, calculations of the equivalent diameter of bubbles which would give such a rising rates were made and compared to the up rising (floating) flocs formed in the FGR (Fig. 14).

Thus, the diameter of the equivalent bubbles calculated by the Stokes equation for the up rising rates of 67 to  $112 \text{ m h}^{-1}$  yielded air bubble sizing between 185 and  $240 \mu\text{m}$ . Because the microbubbles injected were experimentally measured (Rodrigues and Rubio, 2003) and sized between 30 and  $70 \mu\text{m}$ , the only explanation for this phenomenon is the enhanced air volume inside the flocs. Moreover, these values, when compared to conventional DAF are much higher, meaning that using the FGR as bubbles-flocs contactor may lead to a very high capacity floater device. Some authors (Da Rosa, 2002; Haarhoff and Edzwald, 2001; Rubio et al., 2002; Rubio, 2003) explain this phenomenon in terms of the probability of the bubbles, occluded or entrapped, to coalesce in the interior of the flocs.

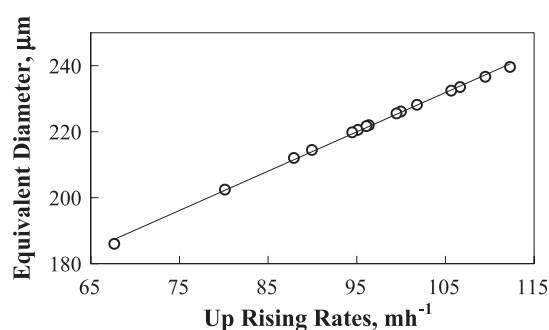


Fig. 14. Equivalent diameter of bubbles as a function of the up rising rate (values obtained with the aerated flocs).

#### 4. Conclusions

An innovative in-line flocculation “helical” unit, named flocs generator reactor (FGR), was developed for the generation of polymeric (aerated and non-aerated) flocs. The studies showed high efficiency for the generation of  $\text{Fe}(\text{OH})_3$  flocs with the employment of a cationic high molecular weight polymer. The polymer flocs obtained were well structured, big and with fractal dimension of 2.98, characteristic of dense flocs, with low porosity and spherical format. The FGR may also be used as a floc-bubble contactor to generate big aerated flocs (5–8 mm). The FGR appear to have some advantages for formation of polymer flocs, namely, a suitable flow mixing, absence of short circuits or dead zones, plug flow profile, low area required, absence of mobile parts, simple design and low mechanical and electrical energy required. Finally, the solid–liquid separation of the flocs by settling reached about  $18\text{--}24\text{ m h}^{-1}$  and more than  $100\text{ m h}^{-1}$  for the aerated flocs. These are values higher than those found in conventional sedimentation tanks or DAF-dissolved air flotation units. It is believed that the FGR appears to have a good potential as a “flocculator” (or flotation) separator device in applications requiring high rate solid–liquid separations.

#### Acknowledgements

Authors thank to the students Silvio Gobbi and Láuren Brondani for their assistance in the experimental work and to all Institutions supporting research in Brazil, especially CNPq (Millennium Project).

#### References

- Adachi, Y., Tanaka, Y., 1997. Settling velocity of an aluminium–kaolinite floc. *Water Research* 31 (3), 449–454.
- Agarwal, S., 2002. Efficiency of shear-induced agglomeration of particle suspensions subjected to bridging flocculation. PhD thesis, West Virginia University, Department of Chemical Engineering, 150 pp.
- Agrawal, S., Nigam, K.D.P., 2001. Modelling of a coiled tubular chemical reactor. *Chemical Engineering Journal* 84, 437–444.
- Akers, R.J., Rushton, A.G., Stenhouse, J.I.T., 1987. Floc breakage: the dynamic response of the particle size distribution in a flocculated suspension to a step change in turbulent energy dissipation. *Chemical Engineering Science* 42 (4), 787–798.
- Austin, L.R., Seader, J.S., 1973. Fully developed vicious flow in coiled circular pipes. *AIChE Journal* 19, 1.
- Bhole, A.G., 1993. Performance of static flocculators. *Proceedings... Chemistry for the Protection of the Environment* 2. Edited by Pawloski et al., IWAQ, 181–194.
- Biggs, S., Habgood, M., Jameson, G.J., Yan, Y., 2000. Aggregate structures formed via a bridging flocculation mechanism. *Chemical Engineering Journal* 80, 13–22.
- Bratby, J., 1980. *Coagulation and Flocculation*. Uplands Press, England. 354 pp.
- Buchanan, I.D., Nicell, J.A., Wagner, M., 1998. Reactor models for horseradish peroxidase-catalysed aromatic removal. *Journal of Environmental Engineering*, 794–802.
- Burns, J.L., Yan, Y.D., Jameson, G.J., Biggs, S., 1997. A light scattering study of the fractal flocculation behavior of a model colloidal system. *Langmuir* 13, 6413–6420.
- Burns, J.L., Yan, Y.D., Jameson, G.J., Biggs, S., 1998. A comparison of the fractal properties of salt-aggregated and polymer-flocculated colloidal particles. *Progress in Colloid and Polymer Science* 110, 70–75.
- Cleasby, J.L., 1984. Is velocity gradient a valid turbulent flocculation parameter? *Journal of Environmental Engineering* 110 (5), 875–897.
- Da Rosa, J.J., 2002. Tratamento de efluentes oleosos por floculação pneumática em linha e separação por flotação: Processo FF. Tese de doutorado em Engenharia, Programa de Pós-Graduação em Engenharia de Minas, Metalúrgica e dos Materiais da UFRGS, 126 pp. (In Portuguese).
- Edzwald, J.K., 1995. Principles and applications of dissolved air flotation. *Water Science and Technology* 31 (3–4), 1–23.
- Elmaleh, J., Jabbouri, A., 1991. Flocculation energy requirement. *Water Research* 25 (8), 939–943.
- Gregory, J., 1981. Flocculation in laminar tube flow. *Chemical Engineering Science* 36 (11), 1789–1794.
- Gregory, J., 1987. Laminar dispersion and the monitoring of flocculation process. *Journal of Colloid and Interface Science* 118 (2), 397–409.
- Gregory, J., 1988. Polymer adsorption and flocculation in sheared suspensions. *Colloids and Surfaces* 31, 231–253.
- Gregory, J., 1997. The density of particle aggregates. *Water Science and Technology* 36 (4), 1–13.
- Gregory, J., 1998. The role of floc density in solid–liquid separation. *Filtration and Separation* 35 (4), 367–371.
- Haarhoff, J., Edzwald, J.K., 2001. Modelling of floc–bubble aggregate rise rates in dissolved air flotation. *Water Science and Technology* 43 (8), 175–184.
- Hüttel, T.J., Friedrich, R., 2000. Influence of curvature and torsion on turbulent flow in helically coiled pipes. *International Journal of Heat and Fluid Flow* 21, 345–353.
- Kiuru, H.J., 2001. Development of dissolved air flotation technology from the first generation to the newest (third) one (DAF in turbulent flow conditions). *Water Science and Technology* 43 (8), 1–7.
- Klimpel, R.C., Hogg, R., 1991. Evaluation of floc structures. *Colloids and Surfaces* 55, 279–288.

- Larue, O., Vorobiev, E., 2003. Floc size estimation in iron induced electrocoagulation and coagulant using sedimentation data. *International Journal of Mineral Processing* 71, 1–15.
- Levenspiel, O., 1999. *Engenharia das Reações Químicas*. Edgar Blücher, 3<sup>a</sup> Edição, São Paulo. 563 pp. (In Portuguese).
- Liers, S., Baeyens, J., Mochtar, I., 1996. Modelling dissolved air flotation. *Water Environment Research* 68 (6), 1061–1075.
- Metcalf, Eddy, 2003. In: Tchobanoglous, George., Burton, Franklin L., Stensel, H. David (Eds.), *Wastewater Engineering: Treatment and Reuse*, 4th edition. McGraw-Hill. 1819 pp.
- Montgomery, D.C., 1991. *Design and Analysis of Experiments*, 3rd edition. John Wiley and Sons, Canada. 649 pp.
- Odegaard, H., Grutle, S., Ratnaweera, H., 1992. An analysis of floc separation characteristics in chemical wastewater treatment. In: Klue, R., Hahn, H.H. (Eds.), *Chemical Water and Wastewater Treatment: II. Proceedings...* 5th Gothenburg Symposium, Nice-França. pp. 247–262.
- Porubská, J., Alince, B., Van De Ven, T.G.M., 2002. Homo and hetero-flocculation of papermaking fines and fillers. *Colloids and Surfaces. A, Physicochemical and Engineering Aspects* 210, 223–230.
- Purchas, D.B., 1977. *Solid/Liquid Separation: Equipment Scale-Up*. Uplands Press Ltd. 584 p.
- Rodrigues, R.T., Rubio, J., 2003. New basis for measuring the size distribution of bubbles. *Minerals Engineering* 16, 757–765.
- Rubio, J., 2003. Unconventional flocculation and flotation. In: Ralston, J., Miller, J., Rubio, J. (Eds.), *Flotation and Flocculation: From Fundamentals to Applications*, Proceedings from Strategic Conference and Workshop, Hawaii, 2002. pp. 17–32.
- Rubio, J., Tessele, F., Porcile, P.A., Marinkovic, E., 2001. Flotación como proceso de remoción de contaminantes: I. Principios básicos, técnicas y aplicaciones. *Minerales* 56 (242), 9–18. (In Spanish).
- Rubio, J., Souza, M.L., Smith, R.W., 2002. Overview of flotation as a wastewater treatment technique. *Minerals Engineering* 15, 139–155.
- Shannon, W.T., Buisson, D.H., 1980. Dissolved air flotation in hot water. *Water Research* 14 (7), 759–765.
- Streeter, V.L., 1961. *Handbook of Fluid Dynamics*, 1st edition. McGraw-Hill Book, New York.
- Tang, P., Greenwood, J., Raper, A., 2002. A model to describe the settling behavior of fractal aggregates. *Journal of Colloid and Interface Science* 247, 210–219.
- Thomas, D.N., Judd, S.J., Fawcett, N., 1999. Flocculation modelling: a review. *Water Research* 33 (7), 1579–1592.
- Weber J., W.J., 1972. *Physicochemical processes for water quality control*. Wiley-Interscience, New York-USA. John Wiley and Sons 640 pp.
- Weir, S., Moody, G.M., 2003. The importance of flocculant choice with consideration to mixing energy to achieve efficient solid/liquid separation. *Minerals Engineering* 16, 109–113.
- Yeung, A., Pelton, R., 1996. Micromechanics: a new approach to studying the strength and breakup of flocs. *Journal of Colloid and Interface Science* 184, 579–585.
- Yeung, A., Gibbs, A., Pelton, R., 1997. Effect of shear on the strength of polymer-induced flocs. *Journal of Colloid and Interface Science* 196, 113–115.
- Yukselen, M.A., Gregory, J., 2003. The reversibility of floc breakage. *International Journal of Mineral Processing* 73 (2–4), 251–259.